Polymeric Dispersants Delay Sedimentation in Colloidal Asphaltene Suspensions

ARTICLE *in* LANGMUIR · MARCH 2010

Impact Factor: 4.46 · DOI: 10.1021/la9049204 · Source: PubMed

3 AUTHORS, INCLUDING:

Sara M Hashmi
Yale University
37 PUBLICATIONS **384** CITATIONS

SEE PROFILE

Langmuir
Article
pubs.acs.org/Langmuir

Polymeric Dispersants Delay Sedimentation in Colloidal Asphaltene Suspensions

Sara M. Hashmi, Leah A. Quintiliano, and Abbas Firoozabadi*

Department of Chemical Engineering, Yale University, New Haven, Connecticut 06510

Received December 31, 2009. Revised Manuscript Received March 15, 2010

Asphaltenes, among the heaviest components of crude oil, can become unstable under a variety of conditions and precipitate and sediment out of solution. In this report, we present sedimentation measurements for a system of colloidal scale asphaltene particles suspended in heptane. Adding dispersants to the suspension can improve the stability of the system and can mediate the transition from a power-law collapse in the sedimentation front to a rising front. Additional dispersant beyond a crossover concentration can cause a significant delay in the dynamics. Dynamic light scattering measurements suggest that the stabilization provided by the dispersants may occur through a reduction of both the size and polydispersity of the asphaltene particles in suspension.

Introduction

Asphaltenes do not have a precise chemical definition; instead they are defined as the fraction of crude oil which is insoluble in light alkanes such as heptane and soluble in aromatic solvents such as toluene. Instability in asphaltene suspensions can arise due to a number of factors including pressure, temperature, and composition. This instability can be problematic in operational situations, and robust methods to delay or prevent instability are much sought after by the oil industry. At the same time, the situations which give rise to asphaltene instability are also those in which asphaltene behavior is the least well characterized or understood from physical or theoretical perspectives. On the lab scale, asphaltene instability often begins with the onset of insolubility, followed by the formation of colloidal scale particles which aggregate and ultimately sediment out of solution. The time required for asphaltenes to fully separate can increase based on solvent composition, indicating that the delay of instability is possible.[1−3] However, a full characterization of asphaltene sedimentation remains to be investigated thoroughly. At the same time, measurements of both sedimentation dynamics and sedimentation equilibrium can be powerful tools for investigation. For instance, dynamics are often used for particle-sizing applications.[4,5] Equilibrium concentration profiles can provide a measurement of the osmotic pressure in a system and thus a full thermodynamic characterization.[6,7] In this study, we investigate the sedimentation dynamics of asphaltene suspensions in heptane and the delay induced by the addition of polymeric dispersants.

Sedimentation is a long-studied problem, and intricacies are still being explored even in systems of well-characterized particles. Single particles settle with a constant velocity most strongly determined by particle size.[8] In colloidal suspensions, several other factors including volume fraction, the presence of walls, and interparticle interactions all affect the velocity.[9−11] Regardless of these other effects, sedimentation in colloidal suspensions shares a common feature: over time, two shock fronts appear roughly simultaneously, one from the top of the sample and one from the bottom.[12] Diffusion can slow both the growth of the sediment as well as the velocity of the falling front.[13] Both experiment and numerical work reveal the impact of diffusion on velocity fluctuations in colloidal sedimentation.[14,15] In the absence of diffusion, long-range correlations appear between sedimenting particles.[16] Attractive interactions between particles even at low volume fractions can lead to the formation of networks which span the sample volume.[17] Sedimentation in colloidal gels exhibits qualitatively different behavior from that of hard-sphere colloidal suspensions. Gravitational collapse of the gel networks often occurs with a sudden collapse followed by a much slower decay.[18,19]

The sedimentation of asphaltenes provides additional challenges to a theoretical understanding, given the polydisperse nature of the particles, their amorphous shape, and the participation of resins and other crude molecules at the asphaltene interface. Asphaltenes are polydisperse in many physical parameters, including molecular size and weight and the number of fused carbon rings in each molecule.[20] Molecular asphaltenes are polydisperse with molecular weight anywhere between 700 and

*To whom correspondence should be addressed. E-mail: abbas.firoozabadi@yale.edu.

(1) Murzakov, R. M.; Sabanenkov, S. A.; Bermejo, J. *Chem. Technol. Fuels Oils* **1980**, *16*, 40.
(2) Idem, R. O.; Ibrahim, H. H. *J. Pet. Sci. Eng.* **2002**, *35*, 233–246.
(3) Maqbool, T.; Balgoa, A. T.; Fogler, H. S. *Energy Fuels* **2009**, *23*, 3681–3686.
(4) Yang, F.-S.; Caldwell, K. D.; Giddings, J. C. *J. Colloid Interface Sci.* **1983**, *92*, 81–91.
(5) Schuck, P. *Biophys. J.* **2000**, *78*, 1606–1619.
(6) Piazza, R.; Bellini, T.; Degiorgio, V. *Phys. Rev. Lett.* **1993**, *71*, 4267–4270.
(7) Rutgers, M. A.; Dunsmuir, J. H.; Xue, J.-Z.; Russel, W. B.; Chaikin, P. M. *Phys. Rev. B* **1996**, *53*, 5043–5046.
(8) Batchelor, G. K. *J. Fluid Mech.* **1972**, *52*, 245–268.
(9) Davis, R. H.; Acrivos, A. *Annu. Rev. Fluid Mech.* **1985**, *17*, 91–118.
(10) Brenner, M. P. *Phys. Fluids* **1999**, *11*, 754–772.
(11) Zwanikken, J.; van Roij, R. *Europhys. Lett.* **2005**, *71*, 480–486.
(12) Davis, K. E.; Russel, W. B. *Phys. Fluids A* **1989**, *1*, 82.
(13) Ackerson, B. J.; Paulin, S. E.; Johnson, B.; van Megen, W.; Underwood, S. *Phys. Rev. E* **1999**, *59*, 6903.
(14) Tee, S.-Y.; Mucha, P. J.; Cipelletti, L.; Manley, S.; Brenner, M. P.; Segre, P. N.; Weitz, D. A. *Phys. Rev. Lett.* **2002**, *89*, 054501.
(15) Bergougnoux, L.; Ghicini, S.; Guazzelli, E.; Hinch, J. *Phys. Fluids* **2003**, *15*, 1875–1887.
(16) Segrè, P. N.; Herbolzheimer, E.; Chaikin, P. M. *Phys. Rev. Lett.* **1997**, *79*, 2574–2677.
(17) Manley, S.; Skotheim, J. M.; Mahadevan, L.; Weitz, D. A. *Phys. Rev. Lett.* **2005**, *94*, 218302.
(18) Starrs, L.; Poon, W. C. K.; Hibberd, D. J.; Robins, M. M. *J. Phys.: Condens. Matter* **2002**, *14*, 2485–2505.
(19) Kim, C.; Liu, Y.; Kuhnle, A.; Hess, S.; Viereck, S.; Danner, T.; Mahadevan, L.; Weitz, D. A. *Phys. Rev. Lett.* **2007**, *99*, 028303.
(20) Andreatta, G.; Bostrom, N.; Mullins, O. C. *Langmuir* **2005**, *21*, 2728–2736.

1000 or greater.[20,23] Small angle X-ray and small angle neutron scattering experiments reveal that the size of asphaltenes ranges anywhere between 10 and 125 Å in a variety of stable solvent conditions.[21,22] Despite the broad range of physical parameters, bulk thermodynamic models have been fairly successful in predicting asphaltene solubility in good solvents. Both Flory theory and the solubility parameter are useful in characterizing asphaltenes in toluene, xylene, and other highly aromatic solvents.[24,25]

Systems in which asphaltenes are unstable present additional challenges to a comprehensive understanding of their behavior. The fused aromatic rings comprising asphaltene molecules have an affinity for π stacking and aggregation, often leading to instability in solution.[20,26,27] This aggregation may be induced by imposing changes in temperature or pressure.[21,28] Compositional changes in oil or the addition of poor solvents may also induce asphaltene instability.[29] For instance, molecular asphaltenes can form colloidal scale particles when crude oil is mixed with heptane or combinations of heptane and toluene.[30] Over time, sub-micrometer scale asphaltene particles can aggregate and form flocs up to the order of 10 μm or larger.[31] Asphaltene instability ultimately results in particle formation, aggregation, sedimentation, and even adsorption to solid surfaces.[32] Bulk thermodynamic models require additional adjustable parameters to describe asphaltenes in any of these situations, often becoming empirical in nature.[33,34]

The major operational challenge in dealing with asphaltenes is to prevent conditions in bulk solutions from approaching those favoring asphaltene precipitation. The addition of certain aromatic solvents in bulk volumes can prevent the growth and aggregation of asphaltenes. The nature of molecular asphaltenes in crude oil provides another suggestion: native resins and other more aromatic components of crude oil can stabilize asphaltenes in suspension.[35,36] Indeed, amphiphilic molecules and certain classes of surfactants have been shown to interact favorably with asphaltene molecules for increased stability.[37−39] While polymeric or amphiphilic dispersants may provide metastability only, they may still suffice to address operational issues caused by asphaltenes. Tests of asphaltene dispersants often involve optical density measurements as a method for dispersant selection, but a detailed understanding of the mechanism of dispersant operation remains to be established.[40,41]

In this study, we induce asphaltene instability by adding a poor solvent, heptane, to crude oil and provide metastability to the resulting asphaltene suspensions by adding small amounts of dispersant. We measure the sedimentation which occurs as a result of the instability of the asphaltenes in heptane. The asphaltene sedimentation has some features in common with colloidal sedimentation, ultimately creating an asphaltene-rich phase at the bottom of the sample. Polymeric dispersants impart a degree of metastability to the system and can greatly delay the sedimentation dynamics. We investigate the mechanism of this delay through dynamic light scattering to characterize asphaltene particle size as a function of dispersant concentration. To gain a better understanding of the mechanisms at work, we investigate three dispersants which impart various degrees of metastability and which therefore cause various degrees of delay in the sedimentation dynamics. To provide a comparison with a more well-characterized system, we also present sedimentation results for colloidal suspensions at similar particle sizes and volume fractions and in the same sample geometry. Understanding the mechanisms controlling and delaying sedimentation in asphaltene systems will enable future studies to both develop a more complete thermodynamic understanding of these systems and determine improved methods for imparting stability to asphaltene operations.

Materials and Methods

The chemicals used include the crude oil itself, the asphaltene-inducing solvent, heptane, and a selection of dispersants. We use a crude oil sample from Mexico. The density of the oil is measured using a densitometer (Anton-Paar DMA 5000), and is $\rho_o = 0.87$ g/mL at 27 °C. The density and index of refraction of heptane (HPLC grade, 99.5%, JT Baker) are measured with the densitometer and a refractometer (Atago RX-5000α), with the results being $\rho_h = 0.68$ g/mL and $n_h = 1.384$ both at 27 °C. We obtain proprietary dispersants, labeled 4F and AG, from Lubrizol Corporation, along with basic information about their chemical classifications, specific gravities, and molecular weights. Dispersant 4F is an alkylated phenol with specific gravity 0.91. Dispersant AG is a polyolefin amide alkeneamine with specific gravity 0.94. The number averaged molecular weight is $M_n \sim 4000$ for 4F and $M_n \sim 2000$ for AG. We also obtain a well-characterized surfactant, aerosol-OT, also called AOT, or sodium bis(2-ethylhexyl) sulfosuccinate (Sigma-Aldrich). AOT is an anionic surfactant with molecular weight 445. Stock solutions of the proprietary dispersants are prepared in heptane at 30 000 ppm by weight. The stock solution of the AOT in heptane is prepared at 200 000 ppm by weight (20%).

The asphaltene content of a crude oil is commonly defined by the amount of solids filtered 24 h after sample preparation from a solution of 1 g of oil mixed with 40 mL of heptane.[26,42] We measure the amount of asphaltene in the crude oil via vacuum filtration through 0.2 μm cellulose nitrate membrane filters (Whatman). Oil is mixed with heptane in a ratio of 1 g to 40 mL, and fully mixed by sonication. After 24 h, samples are filtered to measure the asphaltene content. To collect the asphaltenes, the membrane filters are then rinsed with toluene (Sigma Aldrich) and allowed to dry in ambient conditions. For a collection of 15 samples measured in this manner, the asphaltene content of the oil is $f = 0.035 \pm 0.007$ g/g. To further characterize our system as a function of time and added dispersant, several samples of crude oil in heptane are filtered immediately after sample preparation.

(21) Camahan, N. F.; Quintero, L.; Pfund, D. M.; Fulton, J. L.; Smith, R. D.; Capel, M.; Leontaritis, K. *Langmuir* **1993**, *9*, 2035–2044.
(22) Gawrys, K. L.; Blankenship, G. A.; Kilpatrick, P. K. *Langmuir* **2006**, *22*, 4487–4497.
(23) Mansoori, G. A. *J. Pet. Sci. Eng.* **1997**, *17*, 101–111.
(24) Flory, P. J. *Principles of polymer chemistry*; Cornell University Press: Ithaca, NY, 1966.
(25) Fenistein, D.; Barre, L.; Broseta, D.; Espinat, D.; Livet, A.; Roux, J.-N.; Scarsella, M. *Langmuir* **1998**, *14*, 1013–1020.
(26) Spiecker, P. M.; Gawrys, K. L.; Kilpatrick, P. K. *J. Colloid Interface Sci.* **2003**, *267*, 178–193.
(27) Acevedo, S.; Escobar, O.; Echevarria, L.; Gutierrez, L. B.; Mendez, B. *Energy Fuels* **2004**, *18*, 305–311.
(28) Hirschberg, A.; de Jong, L. N. J.; Schipper, B. A.; Meijer, J. G. *SPEJ, S. Pet. Eng. J.* **1984**, *24*, 283.
(29) Oh, K.; Ring, T. A.; Deo, M. D. *J. Colloid Interface Sci.* **2004**, *271*, 212–219.
(30) Kraiwattanawong, K.; Fogler, H. S.; Gharfeh, S. G.; Singh, P.; Thomason, W. H.; Chavadej, S. *Energy Fuels* **2009**, *23*, 1575–1582.
(31) Burya, Y. G.; Yudin, I. K.; Dechabo, V. A.; Kosov, V. I.; Anisimov, M. A. *Appl. Opt.* **2001**, *40*, 4028.
(32) da Silva Ramos, A. C.; Haraguchi, L.; Notrispe, F. R.; Loh, W.; Mohamed, R. S. *J. Pet. Sci. Eng.* **2001**, *32*, 201–216.
(33) Andersen, S. I.; Speight, J. G. *J. Pet. Sci. Eng.* **1999**, *22*, 53–66.
(34) Pazuki, G.; Nikookar, M. *Fuel* **2006**, *85*, 1083–1086.
(35) Pan, H.; Firoozabadi, A. *AIChE J.* **2000**, *46*, 416–426.
(36) Leon, O.; Contreras, E.; Rogel, E.; Dambakli, G.; Acevedo, S.; Carbognani, L.; Espidel, J. *Langmuir* **2002**, *18*, 5106–5112.
(37) Chang, C.-L.; Fogler, H. S. *Langmuir* **1994**, *10*, 1749–1757.
(38) Chang, C.-L.; Fogler, H. S. *Langmuir* **1994**, *10*, 1758–1766.
(39) Leon, O.; Rogel, E.; Urbina, A.; Andujar, A.; Lucas, A. *Langmuir* **1999**, *15*, 7653–7657.
(40) Andersen, S. I. *Energy Fuels* **1999**, *13*, 315–322.
(41) Laux, H.; Rahimian, I.; Butz, T. *Fuel Process. Technol.* **2000**, *67*, 79–89.
(42) Groenzin, H.; Mullins, O. C. *Energy Fuels* **2000**, *14*, 677–684.

Asphaltene suspensions with the dispersants at various concentrations are also filtered to measure asphaltene content after full sedimentation. These additional filtration results are discussed below.

The asphaltenes filtered from the oil−heptane suspensions without dispersant are isolated and dissolved in toluene for density measurements. The density of the asphaltene−toluene mixture is measured at several different concentrations of asphaltenes using the densitometer. The density of the pure asphaltenes is thus measured at $\rho_a = 1.21 \pm 0.03$ g/mL.

For sedimentation measurements, we generate asphaltene suspensions by mixing the crude oil with heptane in 15 mL centrifuge tubes (Falcon). Mixing is obtained by sonication of the sample for 1 min. Samples are also prepared with dispersant: for these samples, the crude oil, heptane, and dispersant as diluted from the stock solution are mixed simultaneously. To isolate the effect of the dispersants on the asphaltene suspensions, we fix the amount of heptane used in all samples at a ratio of 40 mL per gram of crude oil, the standard composition often used to define asphaltene content. Samples are then left undisturbed at room temperature and pressure, and the sedimentation rate observed under ambient conditions. The height of the shock front h is recorded as a function of time t with the aid of a cathetometer, as is typically used in sedimentation measurements.[43−45] Still images of the sedimentation behavior are captured by digital camera and time-lapse videos by digital video camera.

Dynamic light scattering (DLS) is performed on the asphaltene samples using a compact goniometer system from ALV, at a scattering angle $\theta = 90$ and a wavelength $\lambda = 532$ nm. The wave vector $q = 4\pi n \sin(\theta/2)/\lambda = 0.023$ nm^{-1}, where n is the refractive index of the solvent, heptane. Samples prepared for sedimentation measurements require further dilution in order to minimize the effects of multiple scattering. Samples for the DLS measurements are prepared and sonicated as described above, and 250 μL of the resulting suspension is diluted in 4 mL of heptane. DLS measurements are performed immediately, at 27 °C, collecting results every 30 s for 15 min. Data analysis of the scattered light intensity correlations is performed through Matlab and Fortran, and the dependence of asphaltene particle size on dispersant concentration is discussed below.

In order to compare the asphaltene sedimentation behavior to that of a more traditional colloidal system, we obtain three suspensions of monodisperse silica particles from Bang's Laboratories at volume fraction $\phi = 0.05$, each with particles of a different radius, nominally $a = 1.57$, $a = 0.41$, and $a = 0.16$ μm, as provided by the manufacturer.

The silica suspensions are sonicated and the sedimentation rates are measured in 15 mL centrifuge tubes and with the aid of a cathetometer, in the same manner as the asphaltene suspensions. Still images are obtained with a digital camera. Sedimentation rates are measured at the original concentration, $\phi = 0.05$, for the three silica suspensions. The suspension of $a = 1.57$ μm particles is also diluted to $\phi = 0.005$ and $\phi = 0.0005$, and the sedimentation rate measured.

Results

Sedimentation. For samples with little or no added dispersant, asphaltenes sediment very quickly out of solution, with a single shock that falls from the top of the sample. The level of the separation between the asphaltenes and the supernatant starts at the top of the sample, $h_0 \sim 9$ cm, and begins to fall within minutes after sample preparation. The falling front moves quickly in the initial stages, and then the dynamics slow until the front reaches its equilibrium level h_∞. This monotonic settling can be seen in samples without dispersant, as shown in the images in Figure 1a. Falling fronts which exhibit a fast collapse followed by a slow collapse are often seen in weak gels, which compact under the influence of gravity alone.[18] For this reason, we may refer to falling fronts, with monotonically decreasing $h(t)$, as compaction fronts.

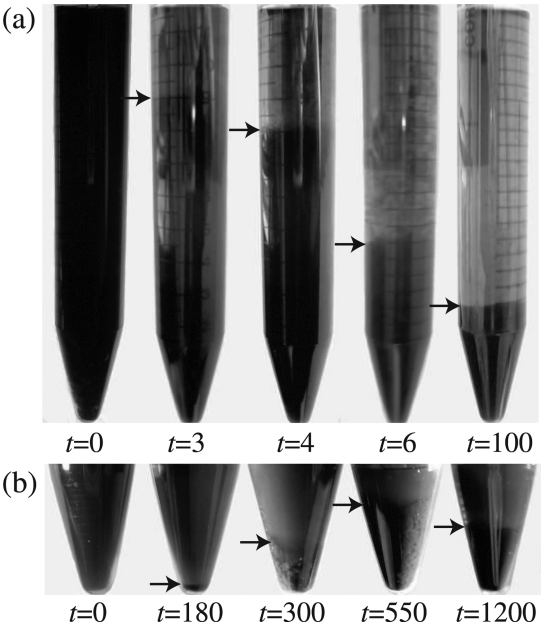

Figure 1. Sedimentation levels of an asphaltene suspension in heptane. The label on each image indicates the time in minutes after fully mixing the sample. The arrows indicate the level of the shock front h. The images in (a) are of a suspension generated by mixing 1 g of crude oil with 40 mL of heptane. In (b), the sample has an additional 500 ppm of dispersant 4F.

Above a characteristic concentration of dispersant, the sedimentation behavior changes qualitatively. Again, a single shock is observed. However, instead of appearing at the top of the sample, the sediment level rises from the bottom of the sample container as the asphaltenes accumulate. Given the finite size of the centrifuge tube, the settling asphaltenes eventually reach the bottom and then pile up on each other, causing the sediment level to grow. The growth of h may begin either minutes or hours after sample preparation, depending on the added dispersant. An example of this behavior is seen in a sample with 500 ppm of dispersant 4F: h first grows to a height above equilibrium and then falls back to h_∞, as shown in Figure 1b.

Samples with varying concentrations of dispersant 4F display the range of observed behaviors. The falling dynamics seen in samples with little or no added dispersant follow a near-power-law behavior, followed by a plateau at h_∞. Sample to sample variation typically causes a scatter in the data of approximately 10%, as seen in the six samples prepared without dispersant and shown in Figure 2a. The solid line shown is the average power-law behavior for the six samples, $h = b\, e^{dt}$. The exponent is obtained by an average of the least-squares fit to each of the six data sets, where $b = 1.24 \pm 0.11$ cm and $d = -0.13 \pm 0.01$ 1/min. When $c =$ 250 ppm of dispersant 4F, the sedimentation behavior changes: h rises from the bottom of the sample instead of falling from the top. Furthermore, h exhibits non-monotonic behavior, with growth followed by collapse. h grows to nearly $2h_\infty$ and then slowly settles to return to h_∞, as seen in Figure 2b. Some samples experience multiple rise−fall events on the millimeter scale in the initial stages

(43) Ray, B. R.; Witherspoon, P. A.; Grim, R. E. *J. Phys. Chem.* **1957**, *61*, 1296–1302.
(44) Phan, S.-E.; Russel, W. B.; Cheng, Z.; Zhu, J.; Chaikin, P. M.; Dunsmuir, J. H.; Ottewill, R. H. *Phys. Rev. E* **1996**, *54*, 6633–6645.
(45) Benes, K.; Tong, P.; Ackerson, B. J. *Phys. Rev. E* **2007**, *76*, 056302.

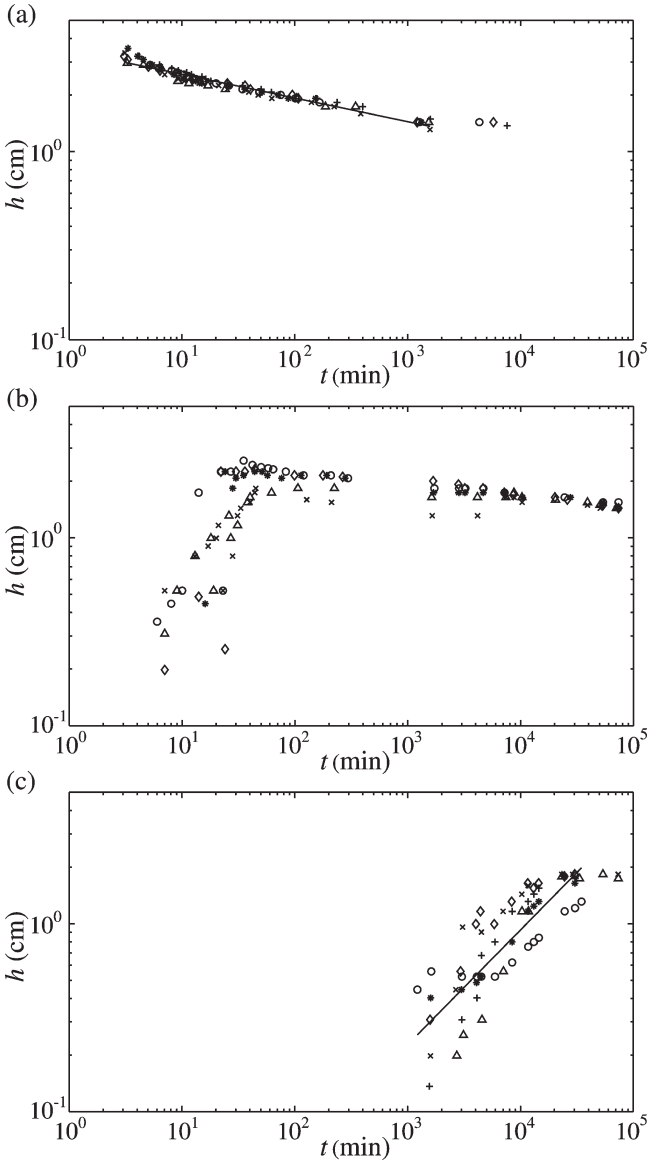

Figure 2. Typical behavior of h seen in asphaltene suspensions. (a) Six samples of asphaltenes in heptane. (b, c) Five and six samples each of asphaltenes in heptane with 250 and 750 ppm of dispersant 4F, respectively. The solid lines in (a, c) denote the average power-law behavior.

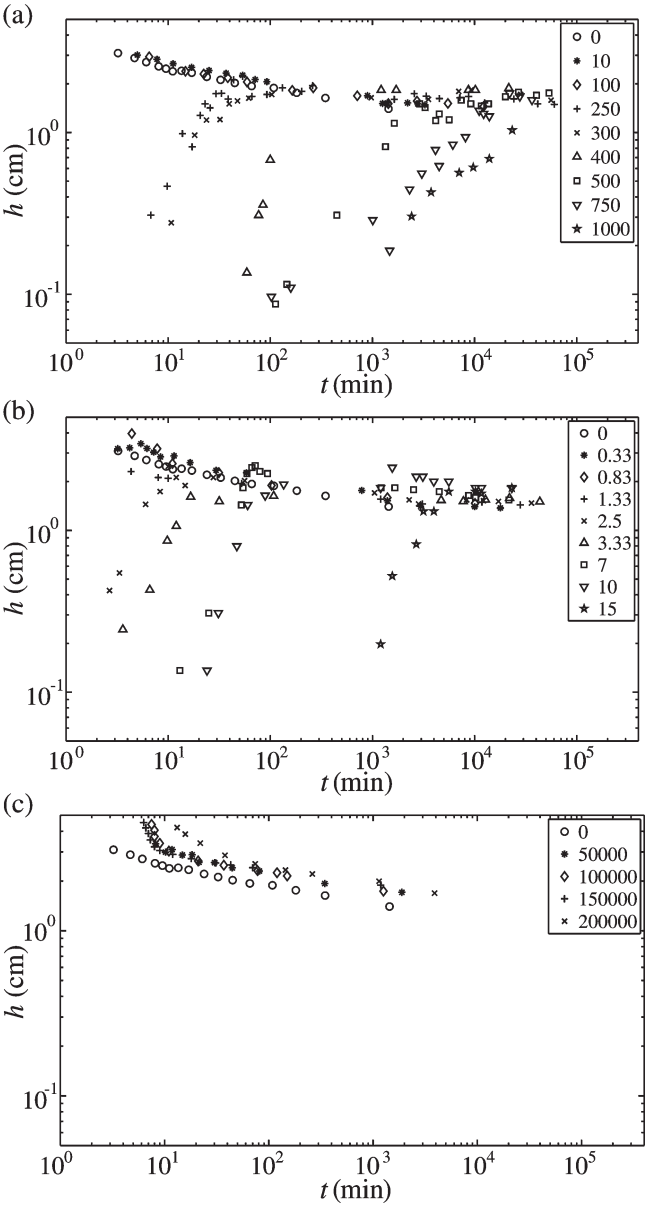

Figure 3. Sedimentation in asphaltene suspensions in heptane with added dispersants 4F (a), AG (b), and AOT (c). The legends indicate dispersant concentration in ppm for each data set.

of sedimentation, as seen in the data sets labeled with (×) and (△) in Figure 2b. With 4F present at concentrations $c = 750$ ppm, the dynamics exhibit a rising sedimentation front followed by a plateau at h_∞. This behavior again seems to have near-power-law dynamics. Sample to sample variation is approximately 30%, as seen in the six samples shown in Figure 2c. The solid line shown is the average power-law behavior for the six samples, also fitted to $h = b\,e^{dt}$. The exponent is obtained by an average of the least-squares fit to each of the six data sets, where $b = -5.70 \pm 1.64$ cm and $d = 0.61 \pm 0.18$ 1/min.

Both dispersants 4F and AG facilitate this qualitative shift in sedimentation behavior as a function of concentration: at low concentrations, h falls from the top of the sample while at higher concentrations h rises from the bottom of the sample. We denote by c^* the characteristic concentration above which h rises rather than falls. The main difference between the behavior of 4F and AG is the concentration required to facilitate the crossover in sedimentation behavior from a falling front to a rising front. For 4F, $c^* \sim 250$ ppm, while for AG $c^* \sim 2.5$ ppm. The dynamics of h for samples with different concentrations of 4F and AG are shown in Figure 3a and b. At low concentrations $c < c^*$, sedimentation occurs through a falling front, in suspensions with $c < 250$ ppm 4F or $c < 2.5$ ppm AG. This behavior is monotonic, and equilibration to h_∞ occurs after about 16 h. For all concentrations $c > c^*$, the level of sediment begins at the bottom of the sample. Near the crossover concentration c^*, h exhibits non-monotonic behavior, first growing quickly to as much as $2h_\infty$ and then falling to equilibrium. As concentration increases above c^*, sedimentation becomes delayed by orders of magnitude: the growth of h begins anywhere from 1 to 1000 min after sample preparation. For instance, in samples with $c = 250$ or 300 ppm of 4F, h begins to grow after 5−10 min. Comparable onset of growth in h, at 5−10 min, is seen in samples with AG at c between 2.5 and 7 ppm. With 500 or 750 ppm of 4F in suspension, h does not exhibit any growth until approximately 100 min after sample preparation. The onset of growth in h occurs nearly 20 h after

preparation for suspensions with either 1000 ppm of 4F or 15 ppm of AG. Full equilibration to h_∞ in these samples takes 7 days or more. The amount of sediment at equilibrium, however, does not depend strongly on dispersant concentration: $h_\infty = 1.50 \pm 0.16$ cm, giving a 10% variation between samples. Given that 4F and AG succeed in significantly delaying the sedimentation of the asphaltene suspensions, we classify them as effective dispersants, noting that AG is effective at a much lower concentration than 4F.

While 4F and AG are proprietary dispersants, a wide variety of well-characterized surfactants has also been used in nonpolar suspensions, including AOT, an anionic surfactant known to form reverse micelles in nonpolar solvents such as heptane.[46,47] The reverse micelles formed by AOT can act as charge carriers, thereby imparting charge to colloids in nonpolar solvents and stabilizing them against aggregation.[48,49] We therefore also test the ability of this commonly available surfactant to stabilize asphaltene suspensions in heptane. Regardless of the amount of AOT, however, the sedimentation exhibits compaction similar to that seen in the absence of dispersants. This behavior does not change to a rising sedimentation front with increasing concentration, as it does with 4F and AG. Even with 20% by weight of AOT in solution, samples still collapse within the first hour after sample preparation, as seen in Figure 3c. This suggests that for AOT $c^* >$ 200 000 ppm. The inability of AOT to cause significant delay in sedimentation even at high concentration indicates that it is not effective in stabilizing asphaltenes.

With dispersants 4F and AG, while the growth of h becomes delayed with increasing concentration for $c > c^*$, the shape of $h(t)$ seems to remain constant. Furthermore, at $c < c^*$, small amounts of dispersant may cause a delay in the onset of the falling front while still preserving the shape of $h(t)$. These observations suggest that the sedimentation dynamics may be collapsed onto a single curve. We investigate this possibility first with 4F and find that each of the curves $h(t)$ can be scaled by a measured characteristic time τ_{sed} which depends on c. We choose this time scale to be $h(\tau_{sed}) \sim 2$ cm. When the time axis for each data set is scaled by $\tau_{sed}(c)$, the data sets collapse onto two fronts, one rising and one falling, as shown in Figure 4a. Note that, for 4F, the rising and falling fronts in the scaled data meet at $t \sim \tau_{sed}$. For samples without dispersant and up to $c = 100$ ppm of 4F, $\tau_{sed} = 50$ min. Above $c = 100$ ppm, τ_{sed} begins to grow. For samples with 1000 ppm of dispersant 4F, $\tau_{sed} = 75\,000$ min, a factor of 1500 longer than τ_{sed} at $c = 0$.

We also use $h(\tau_{sed}) \sim 2$ cm to scale the curves for samples with the other dispersants. For AG at $c < c^*$, $\tau_{sed} \sim 50$ min. Above, c^*, τ_{sed} begins to grow, reaching 27 000 min for $c = 15$ ppm. At $c =$ 15 ppm of AG, τ_{sed} is nearly 600 times longer than τ_{sed} at $c = 0$. Scaling by τ_{sed} for samples with dispersant AG reveals that the meeting of the falling and rising sedimentation fronts occurs at $t < \tau_{sed}$, as seen in Figure 4b. This indicates slightly faster dynamics for samples with dispersant AG as compared with 4F. Although AOT does not stabilize the asphaltene samples as AG and 4F do, the dynamic behavior in these samples also collapses onto a single curve when scaled by $\tau_{sed}(c)$, as seen in Figure 4c. With $c = 200\,000$ ppm of AOT, $\tau_{sed} = 300$ min, 6 times longer than for suspensions without dispersant. Dispersants 4F and AG can delay sedimentation 100−250 times longer than AOT, while at 100−10 000 times lower concentrations.

The behavior seen in the asphaltene suspensions suggests some similarities with sedimentation in colloidal systems. The two fronts

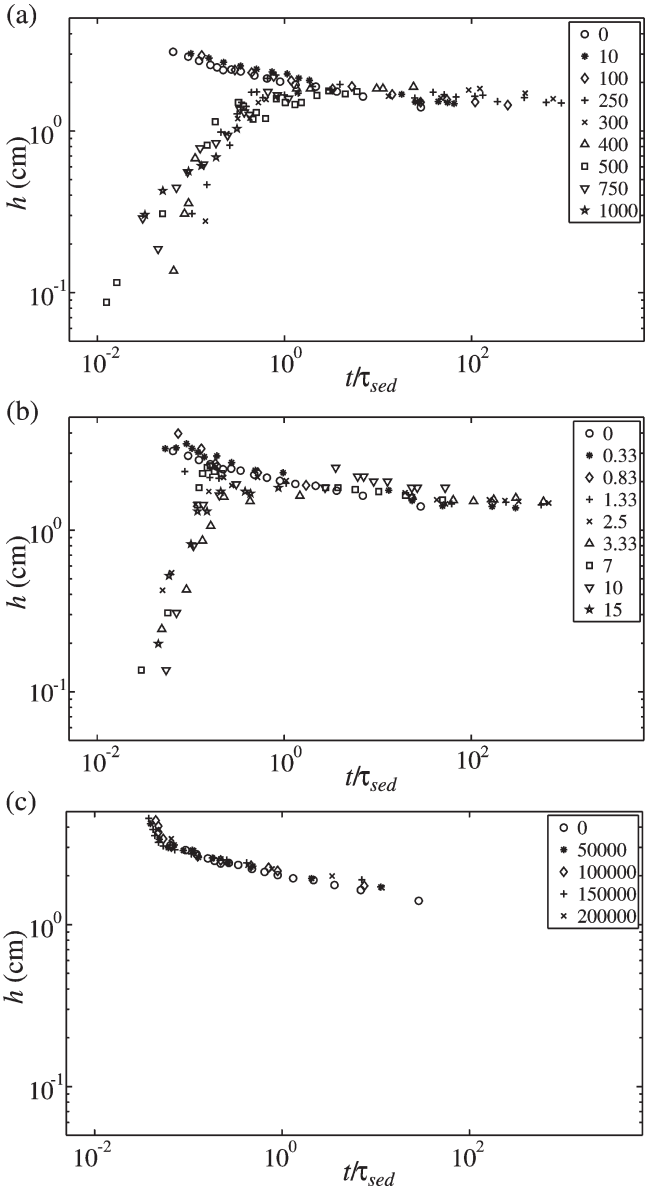

Figure 4. Sedimentation fronts rescaled by the characteristic sedimentation time τ_{sed} for asphaltene suspensions in heptane with dispersants 4F (a), AG (b), and AOT (c). The legends denote the dispersant concentration for each data set.

observed in colloidal sedimentation indicate a separation between the solvent and the liquid dispersion falling from the top of the sample, and the separation between the liquid and a very dense sediment region growing from the bottom.[12] The simplest theoretical formulation of colloidal sedimentation is given by the terminal velocity of a single sphere, the Stokes sedimentation velocity:

$$v_S = \frac{2}{9}\frac{\Delta\rho g a^2}{\mu} \quad (1)$$

where a is the particle radius, μ is the viscosity of the fluid, and $\Delta\rho$ is the density difference between the particle and the fluid. In real systems, many other factors affect sedimentation rate. Hydrodynamic confinement, controlled either by the ratio of particle size to the sample chamber width or by ϕ, can lead to a slowing of the sedimentation velocity by several orders of magnitude[13,50,51]

(46) Jain, T. K.; Varshney, M.; Maitra, A. *J. Phys. Chem.* **1989**, *93*, 7409–7416.
(47) Shirota, H.; Horie, K. *J. Phys. Chem. B* **1999**, *103*, 1437–1443.
(48) Hsu, M. F.; Dufresne, E. R.; Weitz, D. A. *Langmuir* **2005**, *21*, 4881–4887.
(49) Sainis, S. K.; Germain, V.; Mejean, C. O.; Dufresne, E. R. *Langmuir* **2008**, *24*, 1160–1164.
(50) Allain, C.; Cloitre, M.; Wafra, M. *Phys. Rev. Lett.* **1995**, *74*, 1478–1481.
(51) Kuusela, E.; Lahtinen, J. M.; Ala-Nissila, T. *Phys. Rev. E* **2004**, *69*, 066310.

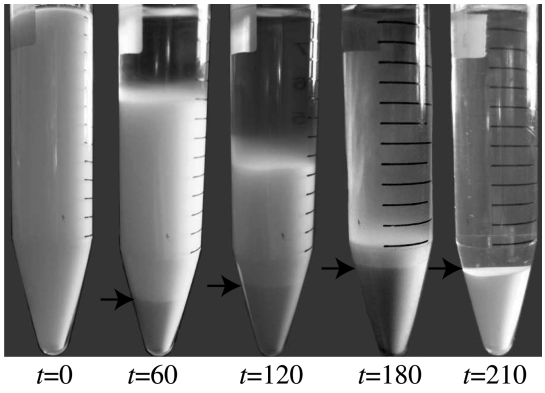

Figure 5. Colloidal sedimentation in a $\phi = 0.05$ suspension of silica spheres of size $a = 1.57\,\mu$m. The label on each image indicates the time in minutes after fully mixing the sample. The white level of the fluid indicates the falling sedimentation front. The arrows indicate the growing sedimentation front.

To assess the effect of the tapered sample geometry used to contain for the asphaltene samples, we use the same sample geometry to observe the sedimentation fronts of a well-defined colloidal system. We vary both ϕ and the particle size in suspensions of silica spheres in water. Both the falling and rising fronts are observed simultaneously in the silica suspensions. This result is shown for the suspension of $a = 1.57\,\mu$m silica particles at $\phi = 0.05$ in the images in Figure 5. The level h falls at a constant velocity which decreases by about 10% as ϕ is increased by 2 orders of magnitude from $\phi = 0.0005$ to $\phi = 0.05$. At $\phi = 0.0005$ the measured, velocity $v = 3.80\,\mu$m/s, falling to $v = 3.50\,\mu$m/s at $\phi = 0.05$. The rising and falling fronts reach h_∞ at the same time, where $h_\infty = 1.83$ cm for the suspension with $\phi = 0.05$ and $h_\infty = 0.48$ cm for $\phi = 0.005$. Both the rising and falling fronts are shown, together with the expectation from the Stokes velocity, in Figure 6a. To assess the effect of geometrical confinement, we vary the particle size at $\phi = 0.05$. As expected from v_S, eq 1, an order of magnitude increase in particle size gives an increase of 2 orders of magnitude in the sedimentation speed: $v = 0.03\,\mu$m/s for $a = 0.16\,\mu$m, $v = 0.23\,\mu$m/s for $a = 0.41\,\mu$m, and $v = 3.50\,\mu$m/s for $a = 1.57\,\mu$m. At $\phi = 0.05$, h falls 2−3 times slower than expected, regardless of a. This can be seen in the semilog plot in Figure 6b, where the solid lines represent spheres falling at v_S for each suspension. The low impact of 1 order of magnitude in a and 2 orders of magnitude in ϕ on v/v_S suggests that the tapered sample geometry does not significantly slow sedimentation.

While the sample geometry of the sample container may not slow sedimentation in the silica suspensions by orders of magnitude, the dispersants may affect ϕ or a in the asphaltene suspensions and thereby facilitate the observed delay. We first estimate the effect of dispersants on the volume fraction of asphaltenes in solution $\phi_a = V_a/V_s$, where V_a is the volume of asphaltenes and V_s the total sample volume. We estimate $V_a = fM_o/\rho_a$ from vacuum filtration measurements, where M_o is the mass of oil used in each sample, f the filtered asphaltene content by weight, and ρ_a the density of the asphaltenes. Immediate filtration of the asphaltene suspensions without dispersant gives $f = 0.05$, suggesting that $\phi_a = 0.0012 \pm 6 \times 10^{-5}$. Filtration further suggests that the amount of asphaltenes decreases by 40% after sedimentation equilibrium, to $f = 0.03$ and therefore $\phi_a = 0.0007 \pm 1.3 \times 10^{-4}$. Dispersant 4F does not strongly affect this result. For a collection of 24 samples with dispersant 4F, three at each concentration measured, filtration gives $\phi_a = 0.0009 \pm 1.6 \times 10^{-4}$, with no

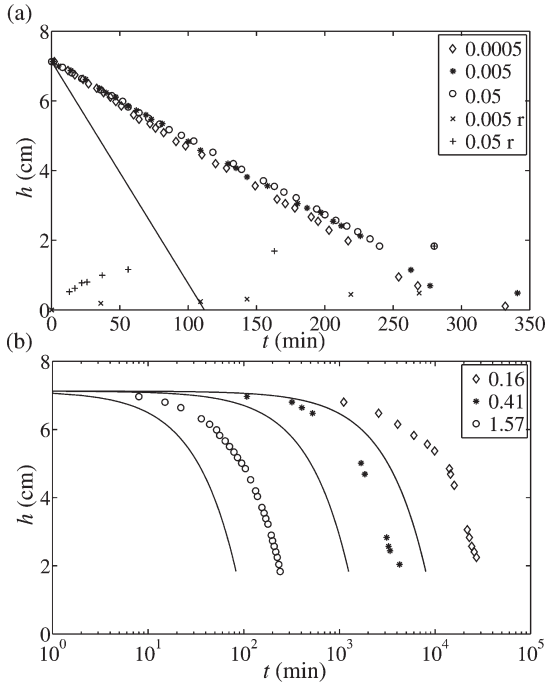

Figure 6. Colloidal sedimentation in the silica suspensions. (a) Three samples of $a = 1.57\,\mu$m sized particles at various ϕ; the ($\times$) and (+) denote the simultaneous rising front in suspensions with $\phi = 0.005$ and $\phi = 0.05$, respectively. (b) Three suspensions of different sized particles, all at $\phi = 0.05$. The solid lines in (a) and (b) indicate the Stokes sedimentation velocity for a single sphere, and (b) is shown on a semilog plot.

systematic dependence on c over the range of concentrations used in the sedimentation samples. Interestingly, the addition of dispersant AG seems to increase the measure of f in suspensions at equilibrium by a factor of 2. Filtration of samples with AG results in $\phi_a = 0.0015 \pm 9^{-5}$ over the range of concentrations measured. However, using the filtration results to estimate V_a ignores the effect of other oil components on the volume of the asphaltenes in suspension.[36] Therefore, we also look at the equilibrium sedimentation level: $h_\infty = 1.50$ cm corresponds to a sedimented volume of $V_a \sim 0.65$ mL. If we assume the asphaltene particles in the sediment are packed near the hard-sphere random close packing limit $\phi_0 = 0.64$, this suggests $\phi_a = \phi_0(V_a/V_s) \sim 0.03$.[52] Using h_∞ estimates that ϕ_a is more than an order of magnitude greater than that suggested by filtration results. Even so, all of these values for ϕ_a still fall within the range of concentrations of the silica suspensions, and they are not strongly affected by dispersant concentration. By comparison with sedimentation in the silica suspensions, it seems unlikely that the differences in the amount of asphaltenes in suspension would give rise to the dramatic delays observed in the sedimentation behavior.

Light Scattering. Since neither sample geometry nor the estimates of ϕ_a can explain the long delay in sedimentation induced by dispersants 4F and AG, we investigate the affect of the dispersants on particle size. We study samples of the asphaltene suspensions using DLS to obtain autocorrelation functions of the scattered light intensity, g, as a function of the lag time (Δt). The exponential decay in $g(\Delta t)$ depends on the translational diffusion time of the system: $\tau_D = 1/2q^2D$, where q is the wave vector and D the diffusivity of the particles in the system. Various fitting methods can be used to extract the decay times from $g(\Delta t)$. For monodisperse suspensions, $g(\Delta t)$ is often fit to an exponential

(52) van Blaaderen, A.; Wiltzius, P. *Science* **1995**, *270*, 1177–1179.

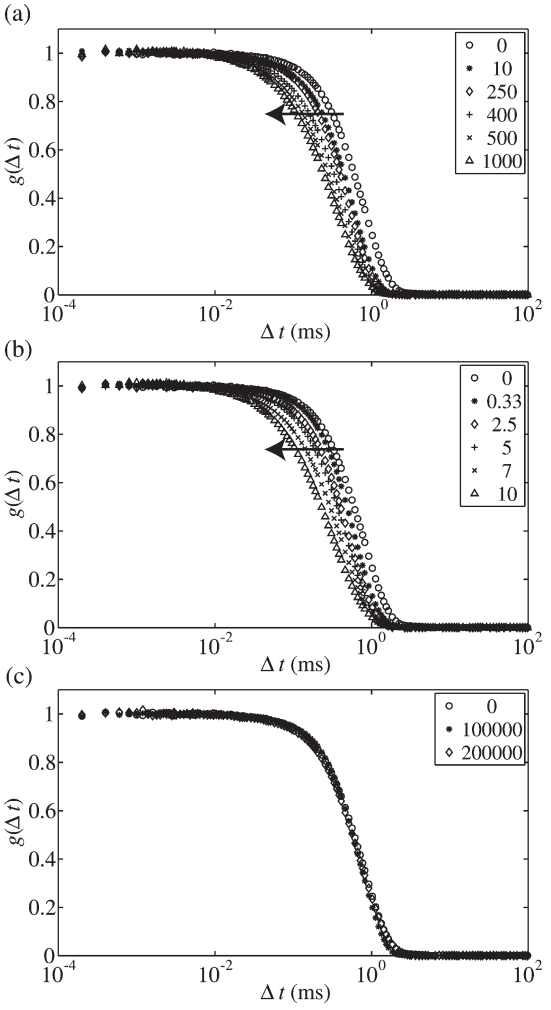

Figure 7. Typical autocorrelation functions of the light intensity scattered from asphaltene suspensions in heptane with added dispersant. Results are shown for selected concentrations of 4F (a), AG (b), and AOT (c). The arrows in (a) and (b) denote increasing dispersant concentration.

function where the exponent is a cumulant expansion to characterize the distribution of Δt.[53] For suspensions which are polydisperse or which have a very broad particlesize distribution, often a better method of fitting involves the Laplace transform:

$$g(\Delta t) = \int p(\tau_D)\, \mathrm{e}^{-\Delta t/\tau_D}\, \mathrm{d}\tau_D \qquad (2)$$

where $p(\tau_D)$ gives the distribution of decay times in the system. The inversion of eq 2 to obtain $p(\tau_D)$ is done numerically, using the freely available CONTIN algorithm.[54,55]

For the asphaltene suspensions in heptane, $g(\Delta t)$ also exhibits a single decay, indicating a monomodal size distribution in these systems as well. The decay in $g(\Delta t)$ reveals the presence of colloidal scale particles immediately after sample preparation, regardless of the concentration of dispersant. Furthermore, the shape of $g(\Delta t)$ remains roughly constant with time, indicating that the particles in dilute solution are stable against both redissolution

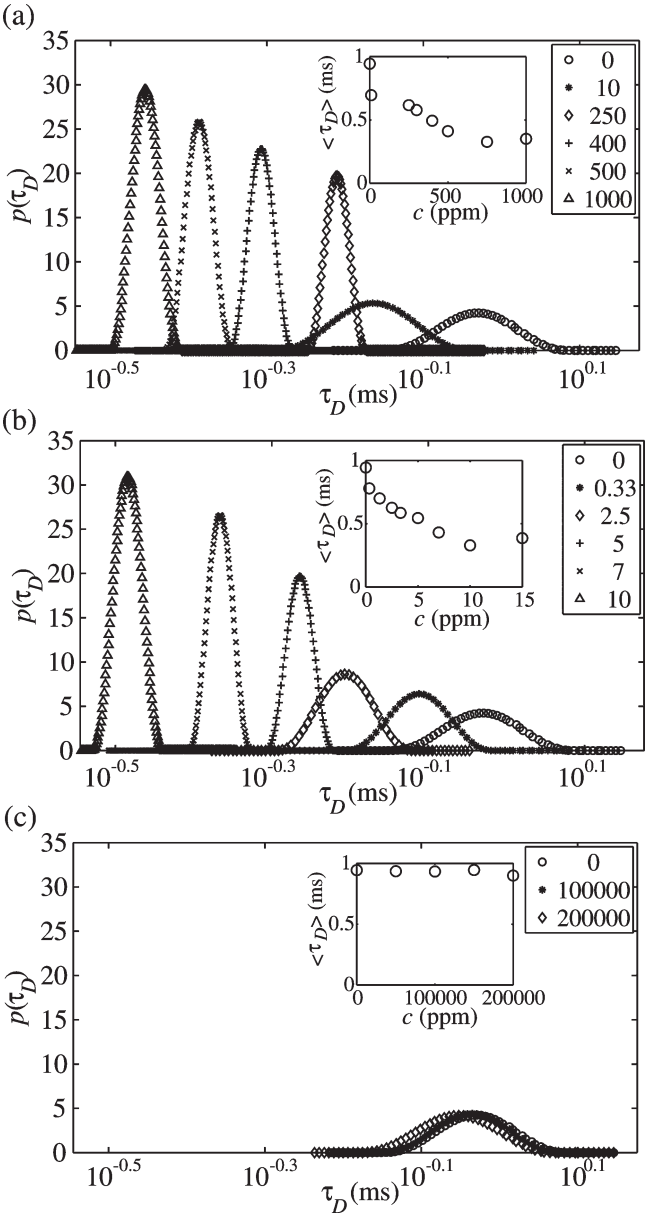

Figure 8. $p(\tau_D)$ for six concentrations of 4F (a) and AG (b), and three concentrations of AOT (c). The insets in each plot show $\langle \tau_D(c) \rangle$ for the range of measured concentrations.

and aggregation. However, as the dispersant concentration increases, the decay time τ_D decreases for samples with both dispersant 4F and AG, as seen in Figure 7a and b. This decrease in τ_D indicates shorter diffusive time scales in the suspensions. However, as the dispersant concentration of AOT is increased in the system, virtually no difference is seen in $g(\Delta t)$, as seen in Figure 7c. For the plots shown in Figure 7, all curves are normalized to $\langle g(\Delta t) \rangle = 1$ for $\Delta t < 0.01$ ms.

Given the natural polydispersity of many asphaltene properties, we use the CONTIN algorithm to fit $g(\Delta t)$ to eq 2 and extract $p(\tau_D)$. Both the type and concentration of dispersant affect $p(\tau_D)$: without any added dispersant, the distribution of decay times is fairly broad. As either dispersant 4F or AG is added to the system, this distribution becomes increasingly narrow, and the peak in p shifts to shorter times. This behavior is seen in the plots of $p(\tau_D)$ for selected concentrations of 4F and AG in Figure 8a and b, respectively. For AOT, however, as seen in $g(\Delta t)$, there is little to no effect of the dispersant on $p(\tau_D)$, as seen in Figure 8c. We

(53) Berne, B. J.; Pecora, R. *Dynamic Light Scattering*; John Wiley and Sons: New York, 1976.
(54) Provencher, S. W. *Comput. Phys. Commun.* **1982**, *27*, 213–227.
(55) Provencher, S. W. *Comput. Phys. Commun.* **1982**, *27*, 229–242.

Table 1. Summary of Dispersant Properties and Main Results for 4F, an Alkylated Phenol, AG, a Polyolefin Alkeneamine, and AOT, an Anionic Surfactant[a]

disp	MW	c^* (ppm)	τ_{sed} (min)	$\langle a \rangle$ (nm)	c (ppm)
4F	4000	250	75 000	210	1000
AG	2000	2.5	27 000	230	15
AOT	445	> 200 000	300	560	200 000

[a] The values of τ_{sed} and $\langle a \rangle$ are those which occur at the value of c in the final column, the maximum concentration used for each dispersant.

calculate the average diffusion time in the system by the first moment of the distribution

$$\langle \tau_D \rangle = \frac{\int \tau_D \, p(\tau_D) \, d\tau_D}{\int p(\tau_D) \, d\tau_D} \quad (3)$$

For both 4F and AG, $\langle \tau_D \rangle$ decreases with concentration, while for AOT there is virtually no change even at very high concentrations, as seen in the insets in Figure 8. The standard deviation σ is given by

$$\sigma^2 = \frac{\int (\tau_D - \langle \tau_D \rangle)^2 \, p(\tau_D) \, d\tau_D}{\int p(\tau_D) \, d\tau_D} \quad (4)$$

As seen in the shape of $p(\tau_D)$, σ also decreases as a function of concentration, from $\sigma = 0.10$ at $c = 0$ to $\sigma = 0.015$ at $c = 1000$ ppm 4F or $c = 15$ ppm AG. In the AOT suspensions, $\sigma \sim 0.10$ even at very high concentrations.

Given that $\tau_D = 1/2q^2D$, if we assume the asphaltene particles are spherical, we can use $D = k_B T/6\pi\mu a$ to extract particle size, where k_B is the Boltzmann constant and T the temperature. Therefore, $\langle \tau_D \rangle$ gives an estimate of the average particle size in suspension $\langle a \rangle = (q^2 k_B T/3\pi\mu)\langle \tau_D \rangle$, and the distribution $p(\tau_D)$ shows the features of the size distribution. The dependence of $p(\tau_D)$ on dispersant concentration indicates that particle size and polydispersity also decrease as a function of concentration. For samples without dispersant, this approximation suggests an average particle size $\langle a \rangle = 600$ nm. This size reduces to $\langle a \rangle = 210$ nm for $c = 1000$ ppm of 4F and $\langle a \rangle = 230$ nm for $c = 15$ ppm of AG. Even at high concentrations of AOT, the decrease in size is modest $\langle a \rangle = 560$ nm at $c = 200\,000$ ppm. The measurements of σ for $p(\tau_D)$ indicate that the polydispersity in the system decreases by nearly an order of magnitude with the addition of 4F or AG but remains constant with AOT. A summary of the main results is listed along with dispersant properties in Table 1.

Discussion

Given this estimation of the average particle size in the system, we can predict the sedimentation behavior for single asphaltene particles in the heptane suspensions. We first determine if the observed sedimentation is expected by calculating the sample Peclet number $Pe = v_S h_0/D$, which indicates the relative importance of sedimentation with respect to diffusion. The measured decrease in τ_D in asphaltene suspensions with dispersants 4F and AG indicates an increase in asphaltene diffusivity with dispersant concentration. In the absence of dispersant, $Pe \sim 10^4$, decreasing to $Pe \sim 10^3$ for the suspensions with 1000 ppm 4F or 15 ppm AG. Since $Pe \gg 1$ in all samples measured, sedimentation does indeed dominate, as observed in these suspensions.

We then use the Stokes velocity, eq 1, to predict the characteristic velocity for sedimentation for a single asphaltene particle, using $\Delta\rho = \rho_a - \rho_h = 0.53$ g/mL. To obtain a prediction for the time scale of sedimentation, we recall that the observed τ_{sed} is defined such that $h(\tau_{sed}) \sim 2$ cm. In the absence of dispersant, given $\langle a \rangle = 600$ nm, the time needed to fall to $h \sim 2$ cm is 1130 min. For both 4F and AG, the predicted sedimentation time increases by nearly an order of magnitude as the dispersant concentration is increased, to 8250 min for $c = 1000$ ppm 4F and 9380 min for $c = 10$ ppm AG. For the AOT suspensions, however, τ_{sed} is predicted to increase only slightly even at $c = 200\,000$ ppm, to 1250 min. The predictions for τ_{sed} are shown by the the asterisk symbol (∗) in Figure 9.

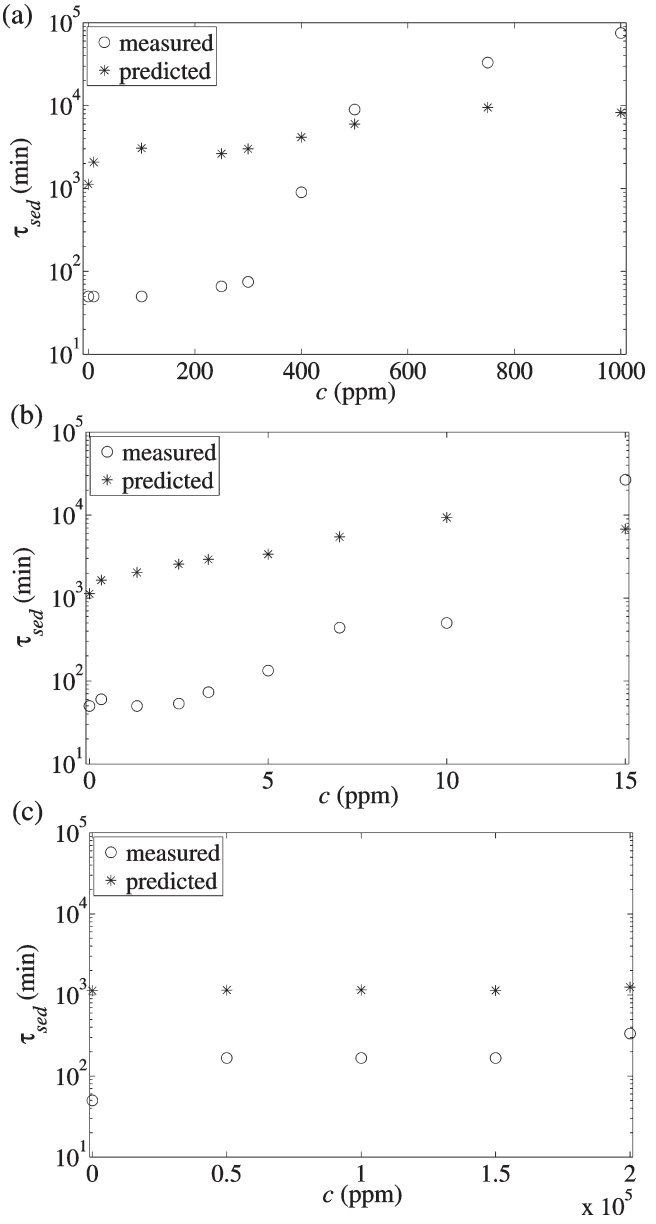

Figure 9. $\tau_{sed}(c)$ for dispersants 4F (a), AG (b), and AOT (c). In each plot, (○) denotes τ_{sed} as measured from sedimentation experiments, while (∗) denotes τ_{sed} as predicted from the particle sizes given by light scattering.

The decrease in the particle size with the addition of dispersants 4F and AG qualitatively predicts the observation that sedimentation slows down with additional dispersant. However, the single particle sedimentation times are more than an order of magnitude slower than those observed in the bulk asphaltene suspensions with $c < 300$ ppm 4F or $c < 5$ ppm AG. Above those concentrations, the bulk sedimentation time begins to approach that predicted by the particle size. At $c > 400$ ppm 4F, the bulk sedimentation time is within an order of magnitude of the

predictions. At c = 1000 ppm 4F and c = 15 ppm AG, the respective settling rates are 9 and 3 times slower than predicted based on the single particle estimate. For all measured concentrations of AOT, the sedimentation in the bulk occurs faster than predicted given the particle size. This comparison can be seen in Figure 9, where the measurements of τ_{sed} in the bulk suspensions are shown by the circle symbol (○).

The combination of the bulk sedimentation measurements together with the light scattering measurements may suggest an explanation for the very fast settling observed with little or no dispersant. With dispersants 4F and AG at $c < c^*$, the bulk sedimentation occurs in a nonlinear fashion, with a power law decrease in $h(t)$. Aggregation is known to speed up the sedimentation process, resulting in nonlinear behavior with a slow settling regime followed by a fast settling regime.[50] Based on the measured sedimentation behavior alone, the power law decrease in $h(t)$ observed at $c < c^*$ suggests that aggregation may be present in these samples. This suggestion is corroborated by the comparison with the predictions based on particle size. The DLS measurements are performed in a dilute solution and therefore reveal simply the asphaltene particle sizes. However, back scattering techniques in concentrated samples show that asphaltene particles can aggregate into flocs of particles within a few hours of sample preparation, signifying diffusion limited aggregation.[31] Aggregation of asphaltene nanoparticles is also revealed by small angle neutron scattering in incompatible crude blends.[57] Aggregation of the asphaltene particles in the sedimentation samples at $c < c^*$ would also explain the discrepancy between the predicted and measured sedimentation times. For instance, at $c = 0$, the particle size is $\langle a \rangle$ = 600 nm, but aggregates of a few or several particles of this size would sediment many times faster than a single one.

If aggregation is present in samples below $c = c^*$, then the effect of the dispersants 4F and AG may be to suppress this aggregation. Indeed, at higher concentrations, $c > 300$ ppm 4F and $c > 5$ ppm AG, the observed sedimentation time in the bulk suspensions approaches the prediction based on the single particle settling rate. Furthermore, as evidenced by the silica suspensions, we do not expect the predictions of τ_{sed} to match the observed behavior in a suspension of particles. While the possibility of aggregation in the absence of dispersants suggests attractive interparticle interactions, slower than expected settling may suggest repulsive interactions, which are known to slow sedimentation.[56] The combination of these observations suggests that, while 4F and AG allow for the formation of colloidal scale asphaltene particles, both are effective in suppressing further aggregation beyond the single particle scale, and in this way act to greatly slow sedimentation in asphaltene suspensions. All samples with AOT both sediment with a power-law behavior and sediment faster than expected considering the size of the single particles, suggesting that AOT may not significantly inhibit further aggregation.

Conclusions

We have characterized the sedimentation behavior of asphaltene suspensions in heptane and with the addition of three dispersants. Without the addition of dispersants, the sedimentation of the asphaltenes occurs quite rapidly, with full separation achieved in approximately 16 h. The results show that the addition of proprietary dispersants 4F and AG to asphaltene suspensions can greatly delay the onset and completion of sedimentation while still allowing the formation of colloidal scale asphaltene particles. This finding suggests that bulk dosing of solvents may not be required to fully prevent asphaltene separation; appropriate dispersants may be used instead to delay intermediate stages of precipitation, such as particle aggregation and sedimentation, long enough for operational purposes. The addition of effective dispersants also affects both the average particle size and the particle size distribution in suspension. When 4F or AG is added to the asphaltene suspensions, the distribution of particle sizes becomes increasingly uniform and distributed around an increasingly smaller average. The decrease of the particle size with increasing dispersant concentration predicts a lengthening of the characteristic sedimentation time.

While the decrease in particle size with additional dispersant may qualitatively explain the delay in sedimentation, several interesting features remain in the sedimentation behavior. Sedimentation at low dispersant concentrations in fact happens nearly 20 times more rapidly than expected. Furthermore, the settling occurs with near-power-law dynamics, with the rate of settling slowing over time. This nonlinear behavior is somewhat similar to the gravitational collapse of gels or the settling of aggregated colloids.[17,50] As the concentration of effective dispersants is increased in suspension, the fast settling no longer occurs, giving way to a rising sedimentation front in its place. At concentrations which suppress the power-law settling behavior, the sedimentation time also begins to approach that predicted by the single particle sizes. The addition of dispersant may therefore facilitate a transition from an aggregated system or interconnected network of particles to a suspension of more isolated colloids. This suggests that asphaltene suspensions may be an interesting system for rheological study. At effective concentrations of 4F and AG, the observed sedimentation time becomes greater than that predicted by single particle size considerations alone. These findings suggest that dispersants may affect other aspects of the suspensions, including the interparticle interactions between asphaltene particles.

Acknowledgment. We gratefully acknowledge the support of RERI member institutions, as well as the use of DLS facilities in Menachem Elimelech's lab at Yale. S.M.H. gratefully acknowledges helpful conversations with Chinedum Osuji. We thank Carlos Lira Galeana of IMP-Mexico for providing the crude sample.

List of Symbols

a	particle radius
c	dispersant concentration, superscript $*$ denotes crossover concentration
f	weight fraction of asphaltenes
$g(\Delta t)$	autocorrelation function of scattered light intensity
h	sedimentation front height; subscripts 0 = initial, ∞ = equilibrium
n	index of refraction, subscript h = heptane
q	wave vector, for light scattering
v_S	Stokes sedimentation velocity

Greek Letters

μ	viscosity
ρ	density; subscripts o = oil, h = heptane, a = asphaltenes
τ_D	diffusive time scale, D = diffusivity
τ_{sed}	characteristic sedimentation time, defined as $h(\tau_{sed}) \sim 2$ cm
ϕ	volume fraction; subscript a = asphaltenes

(56) Vesaratchanon, J.; Nikolov, A.; Wasan, D. T. *Ind. Eng. Chem. Res.* **2009**, *48*, 80–84.
(57) Mason, T. G.; Lin, M. Y. *Phys. Rev. E* **2003**, *67*, 050401.